Research Paper
Computational Methods for Differential Equations
http://cmde.tabrizu.ac.ir
Vol. *, No. *, *, pp. 1-12
DOI:10.22034/cmde.2025.64175.2893

Unsteady and velocity-slip effects on laminar boundary layer flow and forced convective heat transfer over a moving wedge

Shrikant Chavaj[1], Md Hanif Page[2], Krishna B Chavaraddi[3,∗], and Priya M Gouder[4]
[1]Regional Research Centre, VTU, Belagavi-590018, India.
[2]Department of Mathematics, KLE Technological University, Hubballli-580 031, India.
[3]Department of Mathematics, S. S. Government First Grade College and P. G. Studies Centre, Nargund-582 207, India.
[4]Department of Mathematics, KLE Technological University,Dr.M.S.Sheshgiri Campus, Belagavi-590008, India.

Abstract

The focus of this study is to examine the effects of velocity-slip on the surface of the moving wedge on the laminar boundary layer flow of a viscous fluid in addition to the heat transfer across the moving wedge. When fluid and solid interact, velocity-slip effects may have a major impact on most industrial applications. It is considered that the mainstream and wedge velocities and the shape of the velocity-slip depend on the distance along the boundary layer wall. These equations offer the essence of a set of ordinary differential equations for the momentum and thermal boundary layer systems. The numerical solutions reveal that when the velocity-slip and unstable parameters increase, the thermal and momentum boundary layers narrow. The momentum boundary layer domain also appears to be reduced due to pressure gradient effects. There is also little variation in the thermal boundary layers as the wall shear stress (skin-friction) and temperature gradient curves grow flat with increasing velocity-slip parameter. The physical mechanisms underlying these remarkable results are further upon.

Keywords. Boundary layers, Heat transfer, Unsteady effects, Velocity-slip parameter, Moving wedge.
2010 Mathematics Subject Classification. 65L05, 34K06, 34K28.

1. Introduction

Due to its widespread practical applications in filament spinning, power generation, the polymer industry, gas turbine rotors, flow measuring and pumping, rotating machinery, information storage, electronic gadgets, and crystal growth, laminar boundary layer flow of a viscous and incompressible fluid has been studied for decades. During these processes, fluid is used to cool the stretched sheet or filaments, as well as to impart other desirable qualities onto the sheet. Controlling the rate at which sheets or filaments stretch is vital. The method of stretching should be slow enough so that the sheet does not break and the end result has the desired quality. It must also ensure that the sheet keeps flat during the process. In a consequence, these sheets/filaments must be drawn in the space between supported porous blocks or Newtonian fluid [1, 2, 11, 31].

Since it has numerous applications such heat exchanger simulation, cooling and heating system design, thermal optimization, and electric fan simulation, the forced convective heat transfer boundary layer flow is taken into consideration. Further applications for forced convection include high-temperature mechanisms, the flow of refined oil through porous rocks, the extraction of energy from geothermal material, the separation of liquids and solids, and more. The flow of heat between a flowing Newtonian fluid and a wedge surface at a different temperature is known as convection heat transfer. Usually, there are two mechanisms involved in the heat exchange from the fluid to the surface or vice versa. First, when an external force is applied, heat is transferred by the motion of fluid particles, which may be generated by a pump, fan, or density gradients. Secondly, heat is transferred by the interaction between

Received: 25 October 2024 ; Accepted: 15 June 2025.
∗ Corresponding author. Email: ckrishna2002@yahoo.com.

the motion of particles and the moving fluid layer subsequent to the moving surface. The temperature adjacent to the surface is certainly the same as the surface when the fluid flows over it. But velocity and temperature away from a surface fail to change. The hydrodynamic and thermal boundary layers, respectively, are reached by a narrow zone where the distribution of temperature and velocity switch from the wedge wall to the free stream [34]. Nakayama et al. [25] addressed the forced convective boundary layer flow of a fluid with associated heat transfer over a flat plate in a highly dense porous medium; the findings of a local comparable approach were higher compared to direct finite-difference solutions. Salleh et al. [32] investigate the steady forced convection stagnation point boundary layer flow and Newtonian heating, taking into account the surface heat transfer that is proportional to a local temperature. Heat transfer and steady stagnation boundary layer flow in a laminar liquid flow caused by a stretched sheet have been analyzed by Bachok et al. [5]. Due to the presence of nanofluid in the porous media and the inclusion of Brownian motion, Khan and Pop [20] have investigated the transmission of heat. Grosan and Pop's [15] numerical analysis of forced convective boundary layer flow of nanofluid and heat transfer over a needle with a wall temperature variation revealed that an increase in the particle volume fraction causes an increase in the thickness of both the thermal and momentum boundary layers. The local Nusselt number, or temperature gradient, is found to be decreasing when the Brownian motion and thermophoresis parameters increase, according to Ibrahim and Shanker's [17] analysis of the effects of thermal radiation caused by stretching sheets in nanofluids and an externally applied magnetic field. boundary layer fluxes caused by forced convection. Thermal diffusion and inclined magnetic field effects on convection flow have been studied by Kaladhar et al. [18]. Their findings indicate that temperature profiles are found to be decreased while velocity profiles are increased. Researchers Sheikholeslami and Chamkha [35] have examined forced convective heat transfer in nanofluid boundary layer flow while taking Marangoni convection and magnetic field into account. Their findings demonstrate that as Marangoni effects increase, it also increases the hydraulic boundary layer's thickness. Through their study of an unsteady convective slip flow of Casson fluid and heat transfer through a permeable vertical plate, Parmar and Jain [28] have demonstrated that the slip-velocity plays a major role in increasing the thickness of the boundary layer. Mishra et al. [22] studied Navier's slip effects on non-Newtonian nanofluid boundary layer flow over a continuously stretching surface using Buongiorno's model with passive control. They found that the results with active control of wall nanoparticles have a greater influence on Nusselt number instead of Brownian diffusion.

On the other hand, the fundamental understanding of Navier assumption is that slip boundary condition must be utilized which is essential in most of the applications and also in both experimental and theoretical studies [9, 10] confirm that the velocity slip occurs when the fluid-solid surface interaction takes place. The slip boundary condition suggests that both slip velocity and velocity gradient have a linear variation on the wall [4, 23, 26, 29, 37]. Nevertheless, there are applications where the velocity-slip condition is not satisfied and is, therefore, replaced by a partial slip condition [14]. Partial velocity slip happens on the boundary when the fluid is particulate, as in foams, emulsions, polymer solutions, suspensions, and so on. When velocity-slip, a phenomenon known as the non-adherence of fluid particles to the stretching boundary occurs, as is seen in several circumstances [33]. By applying the Chebyshev collocation method, Akolade [3] has examined suction/injection, variable thermophysical influence, and squeezing flow of a magnetised Casson fluid model between two discs subject to velocity slip and convective surface conditions. The author has convincingly demonstrated that the results presented are applicable to parallel disc gate valves, piston locomotion in rings, thermoforming, injection moulding, and other related applications. The fluid flow and associated heat transfer via an oscillating plate in a porous media that accounts for thermal diffusion heat production have been studied by Sheikholeslami et al. [35]. Bhattacharyya et al. [7] showed the effect of slip velocity on a uniformly applied magnetic field in a vertical direction to the boundary layer over a flat plate in a porous material. Two-dimensional flow of a viscous fluid over a wedge in a porous medium has recently been examined by Sayyed et al. [33], who took into account the velocity slip condition.

An unsteady flow is usually the start-up motion or allowed impulsively to move from the rest or transition from one state to another which has significant applications such as missile aerodynamics, influtter phenomena that involve wings, in turbomachines, in aircraft reactions to atmospheric variations, propulsion of fish, etc. During the last few years, it has been also a topic of interest in the fields of biomedical engineering (flow through the arteries, etc). However, the unsteady theory is poorly developed compared to a steady flow, mainly because the velocity component depends on an extra independent variable in the problem that increases the mathematical complexity. These unsteady effects in the model significantly alter the nature of the flow response including transient or non-parallel flow effects.

The assumption is made that the pressure gradient in the flow field remains constant in the normal direction, resulting in the pressure distribution being dependent solely on the streamwise direction, denoted as x. The derivation of the pressure distribution may be obtained from the Prandtl unsteady boundary layer equations, as they are dependent on the unsteady variable that governs the mainstream flow [6]. In the context of unsteady laminar two-dimensional flow, it is commonly assumed that the variation of the mainstream flow may be approximated by a power function of the distance. This power function is expressed as $A(t)x^m$, where x represents the distance along the surface of the wedge, and m is a constant parameter. The Blasius flow is observed in the condition of steady flow with $m = 0$, whereas the stagnation point flow is analyzed when $m = 1$. The Falkner-Skan equation is utilized to describe the characteristics of an unstable boundary layer. Dhanak and Duck [12] and Duck et al. [13] have demonstrated that the Falkner-Skan type flows, resulting from boundary layer flows, encompass a wider range of significant flow phenomena. This has been achieved by utilizing the mainstream velocity in the aforementioned formulation. When the pressure gradient in the boundary layer is equal to the gradient of the mainstream flow, a connection could be established between the Prandtl boundary layer equations and the flow under the inviscid flow core. Hence, the aforementioned constant m is now associated with the pressure gradient. The inclusion of the arbitrary parameter m in the governing equation provides an extra factor that contributes to the overall complexity of the problem. When the value of m is less than zero and greater than zero, the flow is associated with an unfavourable and a favourable pressure gradient, respectively. Furthermore, the moving wedge also plays an important role in unsteady boundary layer flow, with a variable pressure gradient. Kudenatti et al. [21] have obtained double solution structures for $m \in [0, 1]$ in their two-dimensional laminar boundary layer flow and forced convection heat transfer. Analogous to the above approximation, the temperature distribution $T(x, t)$ is also approximated as $BA(t)x^{2m-1}$, where B is some constant related to temperature. In this study, we investigate the flow of a boundary layer and the convective heat transfer of a fluid across a wedge surface. Our aim is to examine this phenomenon for all potential values of m, as self-similar solutions to the system have been identified. The subsequent sections of this paper will provide a comprehensive analysis of these solutions.

In the studies of [30, 38] on the classical Falkner-Skan equation obtained from the steady boundary layer equations with the mainstream flow proportional to x^m, it has been shown that the problem admits a self-similar boundary-layer flows. In addition to this, the unsteady boundary layer equations are also expected to admit similarity-type solutions when the mainstream flow is of the same form. It is known that the steady Falkner-Skan equation exhibits interesting boundary layer solutions for different values of m, and some of the solutions are oscillatory in nature [16, 27]. For an unsteady parameter $K \neq 0$, the existence of the unsteady solutions cannot be taken for granted. However, we are less interested in the global nature of the boundary layer, rather we focus more on obtaining the solutions of the problem involving unsteadiness and pressure gradient, and that admit aforementioned class.

The presentation of the paper is as follows. In section 2, we give the mathematical formulation of the problem in question along with detailed derivation, similarity transformations, etc. The nonlinear partial differential equations that model the problem are converted into a system of ordinary differential equations via the suitable similarity transformations. Section 3 is devoted to give the detailed numerical solutions using the standard Keller-box method. The various interesting results will be provided in section 4 followed by the conclusions in section 5.

2. Formulation

The Laminar flow of a viscous fluid and heat transfer over a floating wedge are studied. We employ the Cartesian system, in which $x-$ axis is taken along the stream-wise direction and $y-$axis be normal to it. We have taken into account forced convective heat transfer over a wedge surface, with wedge surface temperature designated by T_w and mainstream temperature denoted by T_∞, and thus it assumes $T_w \gg T_\infty$. This flow is addressed by the following governing equations:

$$\nabla \cdot \boldsymbol{q} = 0, \tag{2.1a}$$

$$\rho\left(\frac{\partial \boldsymbol{q}}{\partial t}+(\boldsymbol{q}\cdot\nabla)\boldsymbol{q}\right)=\nabla P+\mu\nabla^2\boldsymbol{q}, \tag{2.1b}$$

$$\rho C_p\left(\frac{\partial T}{\partial t}+\boldsymbol{q}\cdot\nabla T\right)=k\nabla^2 T, \tag{2.1c}$$

where $\boldsymbol{q}=(u,v)$ denotes the intrinsic velocity vector, u,v are velocities in x,y directions, ρ is the density of the fluid, P denotes pressure, μ is the dynamic viscosity, C_p is the isobaric specific heat, T denotes the temperature and k is the thermal conductivity of the fluid. For flows that have high Reynolds number, viscosity of the fluid is negligible. But, the effect of fluid viscosity remains significant near a narrow region close to the wall of the wedge. This thin layer is technically referred as boundary-layer. Further, for fluids with small thermal conductivity, the heat transfer through conduction is akin to that of convection across a thin layer near the wall, known as thermal boundary-layer. Now, the governing equations are taken in their vector form and then non-dimensionalized by the following variables

$$(x^*,y^*,t^*)=\left(\frac{x}{L},\frac{y}{L},\frac{Ut}{L}\right),\ (u^*,v^*)=\left(\frac{u}{U},\frac{v}{U}\right),\ P^*=\frac{P}{\rho U^2},\ T^*=\frac{T}{\Delta T}, \tag{2.2}$$

where $U,L,\Delta T$ are the suitable reference quantities used to obtain the dimensionless velocity, length and temperature quantities. The boundary-layer scaled version of system (2.1) can be written as

$$\frac{\partial u}{\partial x}+\frac{\partial v}{\partial y}=0, \tag{2.3a}$$

$$\frac{\partial u}{\partial t}+u\frac{\partial u}{\partial x}+v\frac{\partial u}{\partial y}=-\frac{1}{\rho}\frac{\partial P}{\partial x}+\nu\frac{\partial^2 u}{\partial y^2}, \tag{2.3b}$$

$$0=\frac{\partial P}{\partial y}, \tag{2.3c}$$

$$\frac{\partial T}{\partial t}+u\frac{\partial T}{\partial x}+v\frac{\partial T}{\partial y}=\frac{1}{Pr}\frac{\partial^2 T}{\partial y^2}, \tag{2.3d}$$

where $\nu=\frac{\mu}{\rho}$ is the kinematic viscosity and $Pr=\frac{\frac{k}{\rho C_p}}{UL}$ is the ratio of thermal diffusivity to momentum diffusivity, known as Prandtl number, (here * have been dropped for convenience). Further, from Bernoulli's theorem it follows that, for the flow outside the boundary-layer, we have

$$\frac{\partial U}{\partial t}+U\frac{\partial U}{\partial x}+\frac{1}{\rho}\frac{\partial P}{\partial x}=0. \tag{2.4}$$

If U_w denotes the wedge velocity, the boundary conditions the system encompasses are as shown below.

$$\text{when } t<0: u=0,\ v=0,\ T=T_\infty, \tag{2.5a}$$

$$\text{when } t>0: u=U_w(x,t)+N\mu\frac{\partial u}{\partial y},\ v=0,\ T=T_w,\ \text{at } y=0, \tag{2.5b}$$

$$u\to U(x,t),\ v=0,\ T\to T_\infty,\ \text{as } y\to\infty\ , \tag{2.5c}$$

here the mainstream velocity outside the boundary-layer ($U(x,t)$) and the wedge velocity ($U_w(x,t)$) are approximated as

$$U(x,t)=U_\infty A(t)x^m,\ U_w(x,t)=U_0A(t)x^m, \tag{2.6}$$

so that self-similar solutions exists. Here U_∞, U_0 are positive constants, $A(t)$ is an arbitrary time function and m is the exponent to which the length coordinate x must be raised in order to obtain similar velocity profiles. Also T_w

denotes the temperature at the wall and T_∞ is the ambient fluid temperature, such that $T_w \gg T_\infty$. We now define the following similarity variables

$$\eta = \sqrt{\frac{(m+1)\,U}{2\nu x}}y,\ \ \psi(x,t) = \sqrt{\frac{2\nu x U}{m+1}}f(\eta),\ \ T = T_\infty + BA(t)x^{2m-1}\theta(\eta), \tag{2.7}$$

which transforms the partial differential equation system (2.3) to a system of nonlinear coupled ordinary differential equation as

$$f''' + ff'' + \beta(1 - f'^2) = K\left(\frac{\eta}{2}f'' + f' - 1\right), \tag{2.8a}$$

$$\theta'' + Prf\theta' - Pr(3\beta - 2)f'\theta = PrK\left(\frac{\eta}{2}\theta'\right), \tag{2.8b}$$

when $u = U(x,t)f'$ and $v = -\sqrt{\frac{(m+1)\ \nu\ U}{2x}}\left(f + \frac{m-1}{m+1}\eta f'\right)$ are defined, which satisfies the continuity equation identically. Further, the boundary conditions takes the from

$$\text{at } \eta = 0\ \ f(\eta) = 0,\ \ f'(\eta) = \lambda + Nf''(\eta),\ \ \theta(\eta) = 1, \tag{2.9a}$$

$$\text{as } \eta \to \infty\ \ f'(\eta) = 1,\ \ \theta(\eta) = 0, \tag{2.9b}$$

where $\beta = \frac{2m}{m+1}$ is the pressure gradient parameter, whose non-negative values denotes the flow is accelerated and decelerated otherwise. Also $\lambda = \frac{U_0}{U_\infty}$ is termed as the velocity ratio parameter, it signifies direction and speed with which the wedge moves relative to freestream. If $\lambda = 0$, the wedge is at rest and when $\lambda < 0$ the wedge moves in a direction opposite to that of mainstream and vice-versa. Also when $\lambda > 1$, the wedge moves with a velocity faster to mainstream and on contrary the freestream moves rapidly than the wedge if $\lambda < 1$. K is known as the unsteady parameter defined as $K = (2-\beta)\frac{U_\infty^{m-2}}{\nu^{m-1}}\frac{A'(t)}{A^2(t)}$.

The boundary conditions on the velocity component given in (2.9) are such that the fluid velocity on the wedge surface decays under the influence of velocity-slip to the mainstream. In a manner quite similar, the temperature of the fluid that is on the surface of the wedge gradually decreases until it reaches the temperature of the mainstream some distance from the wedge.

Thus, the system (2.8)-(2.9) describes the forced convective heat transfer and the boundary layer flow over a moving wedge in which the velocity-slip is also considered. Since the system (2.8)-(2.9) is highly nonlinear, any analytical solution is not possible; we thus solve it numerically using the standard Keller-box method. A brief description of the method is given in section 3.

3. Numerical procedure: Keller-box method

The above nonlinear problem has no analytical solution feasible; we therefore seek its solution by a numerical procedure. We employ a finite difference-based technique which is often known as box method or Keller-box method is fast and efficient technique which is unconditionally stable and has second order convergence[8, 19]. Keller-box technique is a hybrid technique which employs finite difference method, Newton linearization and the factorization method for its execution. The total fifth-order(3+2) equation is converted to five first order and coupled differential equations by introducing the following variables

$$\frac{df}{d\eta} = \mathcal{H},\ \ \frac{d\mathcal{H}}{d\eta} = \mathcal{S} \text{ and } \frac{d\theta}{d\eta} = \mathcal{T}, \tag{3.1}$$

as

$$\mathcal{S}' + f\mathcal{S} + \beta\left(1 - \mathcal{H}^2\right) = K\left(\frac{\eta}{2}\mathcal{S} + \mathcal{H} - 1\right), \tag{3.2a}$$

$$\mathcal{T}' + Prf\mathcal{T} - Pr\,(3\beta - 2)\,\mathcal{H} = PrK\frac{\eta}{2}\mathcal{T}, \tag{3.2b}$$

and the respective boundary conditions are given by

$$f(0) = 0,\ \mathcal{H}(0) = \lambda + N\mathcal{S}(0), \theta(0) = 1, \tag{3.3}$$

$$\mathcal{H}(\infty) = 1, \theta(\infty) = 0. \tag{3.4}$$

Applying finite difference approximations using backward differences , we obtain

$$f_i - f_{i-1} = d(\mathcal{H}_i + \mathcal{H}_{i-1}), \tag{3.5a}$$

$$\mathcal{H}_i - \mathcal{H}_{i-1} = d(\mathcal{S}_i + \mathcal{S}_{i-1}), \tag{3.5b}$$

$$\theta_i - \theta_{i-1} = d(\mathcal{T}_i + \mathcal{T}_{i-1}). \tag{3.5c}$$

therefore, system (3.2) takes the form

$$(\mathcal{S}_i - \mathcal{S}_{i-1}) + \frac{d}{2}(f_i + f_{i-1})\,(\mathcal{S}_i + \mathcal{S}_{i-1}) + \frac{d\beta}{2}\left(4 - (\mathcal{H}_i + \mathcal{H}_{i-1})^2\right) - K\left(id^2\,(\mathcal{S}_i + \mathcal{S}_{i-1}) + d\,(\mathcal{H}_i + \mathcal{H}_{i-1}) - 2d\right) = 0, \tag{3.6a}$$

$$(\mathcal{T}_i - \mathcal{T}_{i-1}) + Pr\frac{d}{2}(f_i + f_{i-1})\,(\mathcal{T}_i + \mathcal{T}_{i-1}) - Pr(3\beta - 2)d\,(\mathcal{H}_i + \mathcal{H}_{i-1}) = PrKid^2\,(\mathcal{T}_i + \mathcal{T}_{i-1}), \tag{3.6b}$$

for $j = 1, 2, \cdots, M-1$, where M is number of grid points in the boundary-layer domain, $d = \frac{\Delta\eta}{2}$, $\Delta\eta$ is the grid size in η direction. The above system (3.5)-(3.6) produces a nonlinear algebraic system of equations which is tedious to solve. We, therefore, linearize them using Newton's Linearization technique

$$[\mathbf{a}]^{(k+1)} = [\mathbf{a}]^{(k)} + [\delta\mathbf{a}]^{(k)}, \tag{3.7}$$

where

$$\mathbf{a} = \left[\begin{array}{ccccc} f & \mathcal{H} & \mathcal{S} & \mathcal{T} & \theta \end{array}\right]^{tr}. \tag{3.8}$$

Substituting (3.7) into the system (3.5)-(3.6) and dropping quadratic and higher-order terms we obtain a system of linear algebraic equations. This linearized difference equation of the above system has a block tri-diagonal structure. In the vector form, it can be represented in matrix form as

$$\mathbf{AD} = \mathbf{R}. \tag{3.9}$$

The tridiagonal structure of (3.9) can be solved by using the factorization method. The solutions $\mathbf{D}$ is updated at each iteration until desired convergence is achieved. The error tolerance is set to 10^{-6} for all the simulations. We performed these simulations with error tolerance 10^{-8}, solutions were indistinguishable. Henceforth, we continued with 10^{-6} for all the numerical simulations.

The following are the important derived quantities that are relevant to the present study which are given by the skin friction co-efficient C_f and the Nusselt number Nu_x (temperature gradient) and are given by

$$C_f = \frac{\tau_w}{\rho U^2} \text{ and } Nu_x = \frac{xq_w}{\lambda(T_w - T_\infty)}, \tag{3.10}$$

where the shear stress τ_w and the heat transfer q_w are given by

$$\tau_w = \mu\left(\frac{\partial u}{\partial y}\right)_{y=0} \text{ and } q_w = -\alpha\left(\frac{\partial T}{\partial y}\right)_{y=0}, \tag{3.11}$$

with α is the specific heat conductivity and μ is the fluid viscosity. Accordingly, we have

$$C_f = \frac{\mu}{\rho}\left(\frac{(m+1)U}{2\nu x}\right)^{\frac{1}{2}} f''(0),\ \text{and}\ \ Nu_x = \left(\frac{(m+1)xU}{2\nu}\right)^{\frac{1}{2}} \theta'(0), \tag{3.12a}$$

where both $f''(0)$ and $\theta'(0)$ are determined the above system and these effects shall be discussed later.

4. Results and discussion

In the present section, we discuss various results obtained for the system (2.8)-(2.9) numerically by Keller-box technique. We have computed the quantities of engineering interest such as velocity profiles ($f'(\eta)$), temperature profiles $\theta(\eta)$, wall shear stress $f''(0)$ and Nusselt number $\theta'(0)$ for a varying range of parameters $K,\ \lambda,\ N,\ \beta,\ Pr$.

We now discuss the velocity and temperature profiles obtained numerically for different values of the unsteady parameter K while keeping other parameters constant. Figure 1 displays these quantities. Note that $K = 0$corresponds to the solutions of the Falkner-Skan flow problem. We noticed from Figure 1(a) that as the unsteady K increases, the Keller-box method predicts the thinning of the momentum boundary layer compared to the steady flow ($K = 0$). This means that as K increases the velocity of fluid starts to increase and hence adheres to the wedge surface. On the other hand, also from Figure 1(b) is clear that as K increases, the thermal boundary layer thickness becomes thicker. The heat transfer rate is thus enhanced.

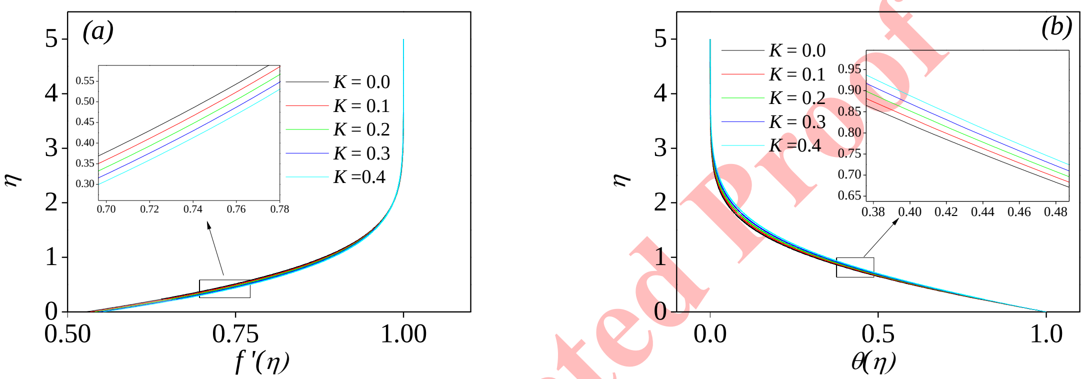

(a) Velocity profiles. (b) Temperature profiles.

Figure 1. Velocity (1(a)) and temperature (1(b)) profiles for different values of the unsteady arameter K at $\lambda = 0,\ Pr = 1,\ \beta = 0.5,\ N = 1$.

Figure 2 shows the variation of the velocity and temperature profiles for different velocity ratio parameters λ while while keeping the other parameters constant. Note that for negative λ (say -1 and -0.5), the wedge is moving opposite to the mainstream flow and vice-versa. When $\lambda < 1$ the wedge velocity is faster than that of the mainstream flow velocity, while $\lambda > 1$ case corresponds to the opposite situation. In each case of λ as shown in Figure 2(a), all the velocity profiles approach the mainstream asymptotically in which when $\lambda < 1$ ($\lambda > 1$) these curves decay to the mainstream from the left (right). Since the wedge and mainstream velocities are equivalent when $\lambda = 1$, no boundary layer arises, and the momentum boundary layer may be described exactly $f(\eta) = \eta$ for all physical parameters. Figure 2(b) shows that the thermal boundary layer is thinner and heat transport is slower than envisaged.

The variations of velocity-slip parameter N on both velocity and temperature distribution are shown in Figures 3(a) and 3(b) respectively. On the account of the velocity-slip, the flow velocity is modified near the wedge surface but approaches asymptotically to mainstream flow. The results are seemingly similar to the solutions given in Figure 2. The effects of velocity-slip are to decrease the thickness of both boundary layers. Mukhopadhyay [24] has noticed similar velocity profiles in a still fluid in the presence of the uniformly applied magnetic field. In the case of temperature profiles, when $N < 0$ there are overshoots near the wedge surface but eventually disappear when N is increased. The thickness of thermal boundary layer is again found to be thinning for increasing N.

To continue, we will look into how the pressure gradient influences the boundary layer flow and the unsteady forced convection heat transfer over a moving wedge. Figure 4(a) depicts the flow trend for favourable pressure gradient β keeping other parameters constant. It is clear that an increasing value of β, increases the flow speed which makes

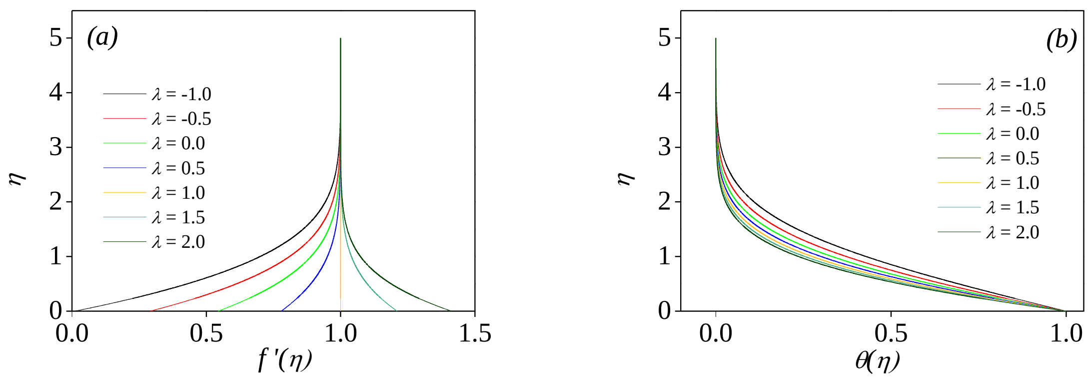

(a) Variation of velocity profiles. (b) Variations in thermal velocity profiles.

FIGURE 2. Variation of velocity and thermal profiles for different λ at $K = 0.25,\ Pr = 1, \beta = 0.5,\ N = 1$.

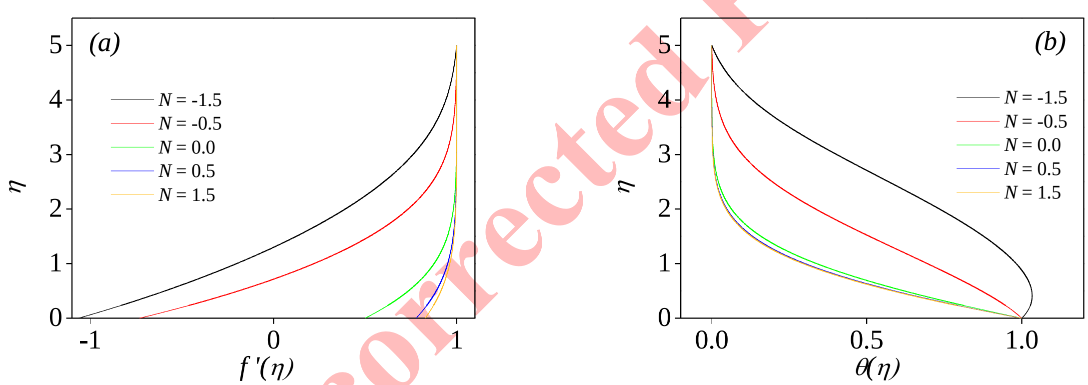

(a) (b)

FIGURE 3. Variation of velocity and thermal profiles for different N at $K = 0.25,\ Pr = 1, \beta = 0.5,\ \lambda = 0.5$.

thinning of the boundary layer thickness. The velocity in the confinement of the boundary-layer approaches that of mainstream asymptotically. Since, the velocity gradient on the surface is a function of both λ and N, the initiation of velocity is rather different for different pressure gradient. On boundary layer thickness increases for enhanced accelerated flows as shown in Figure 4(b). When pressure gradient parameter is as large as 1, there is a overshoot $(\theta(\eta) > 1)$ in the thermal boundary layer which further enhances the heat transfer rate. Fluid velocity increases as viscosity effects increase and temperature lowers. The figure further confirms that the thermal and momentum boundary layer thicknesses are analogous since $Pr = 1$.

We now study the effects of Prandtl number on the forced convection heat transfer. We see that as equation(8a) is independent of Pr, no changes are observed in velocity profiles; hence, have plotted the temperature profiles for varying Prandtl number. The velocity-slip on the surface appears to have little influence on heat transfer. The thermal boundary layer becomes smaller as the Prandtl number increases. In general, the higher the Prandtl number, the bigger

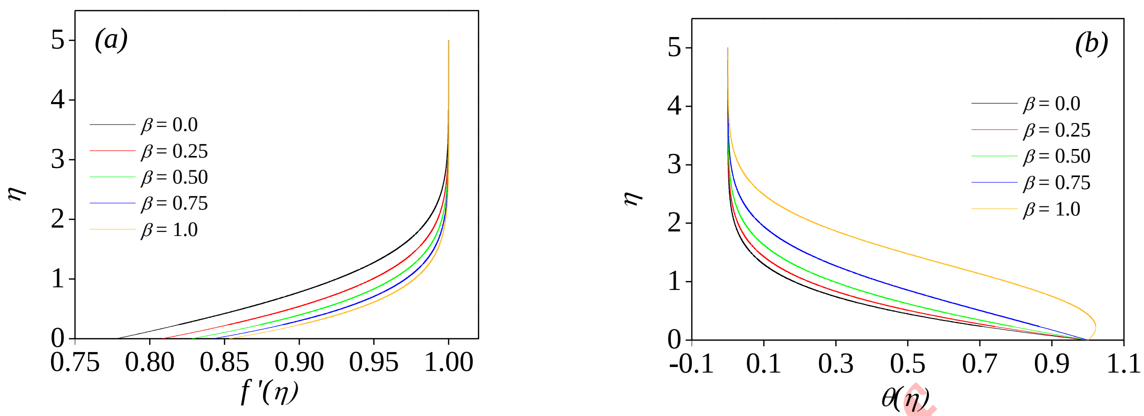

(a) (b)

FIGURE 4. Variation of velocity and thermal profiles for different β at $K = 0.25,\ Pr = 1, N = 1.5,\ \lambda = 0.5$.

the thermal diffusivity relative to momentum diffusivity and, as a result, the quicker the rate of heat transfer. As seen in Figure 5, this typically decreases the thickness of the thermal boundary layer.

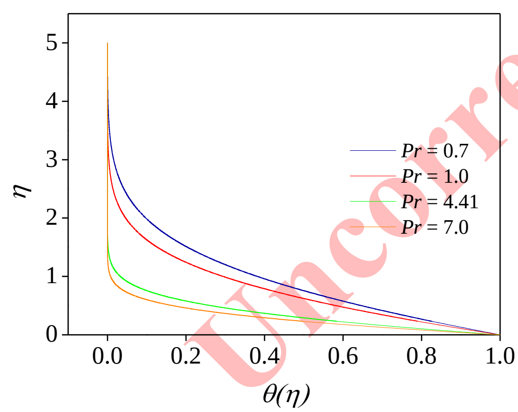

FIGURE 5. Variation of temperature for different values of Prandtl number Pr at $K = 0.25,\ \beta = 0.5, N = 1.5,\ \lambda = 0.5$.

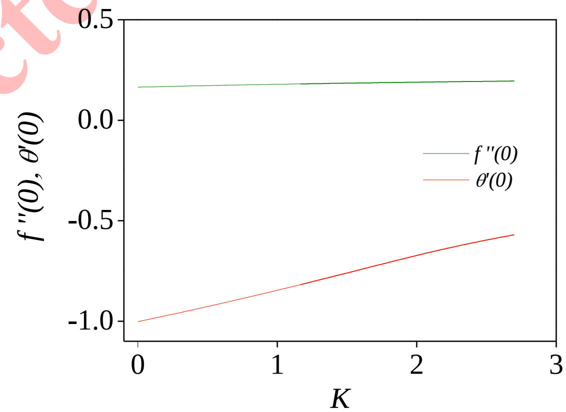

FIGURE 6. Variation of wall shear stress ($f''(0)$) and Nusselt number ($\theta'(0)$) values as a function of unsteady parameter K for $Pr = 1,\ \beta = 0.5, N = 1,\ \lambda = 0.7$.

We now discuss most of our results in a broader structure in terms of the wall shear stress (skin-friction) $f''(0)$ and temperature gradient(Nusselt number) $\theta'(0)$. Figure 6 shows these variations when Pr is increased from zero. It is noticed that, $f''(0)$ is always positive while is negative. The curves for $f''(0)$ is almost flat thereby showing a little variation. The velocity profiles produced in Figure 1(a) can be confirmed that also a little variation in the velocity profiles although $K \in [0, 0.4]$ have been considered.

Figure 7 depicts that there is a variation in $f''(0)$ and $\theta'(0)$ or different values of N. The numerical results show that for negative N values, the visible difference can be seen while for positive N values, both results become almost flat thereby showing a constant variation. Thus, to have the significant velocity-slip effects, the value of N should be sufficiently small in the model. The wall shear stress and the Nusselt number are given in Figure 8 show that when the velocity ratio λ is increased from -1, the decreases gradually to a negative infinity while varies marginally. Because the mainstream flow velocity is significantly faster than the wedge velocity, the skin-friction is always decreasing. This is due to the fact that the wedge velocity is significantly lower. When λ increases, there is a gradual enhancement in the heat transfer.

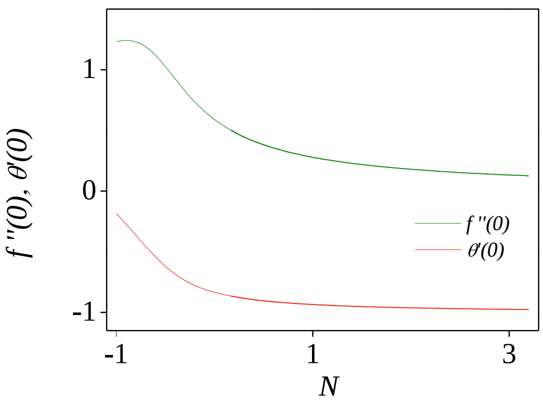

Figure 7. Variation of wall shear stress ($f''(0)$) and Nusselt number ($\theta'(0)$) values as a function of Knudsen number N for $Pr = 1,\ \beta = 0.5, K = 0.25,\ \lambda = 0.5$.

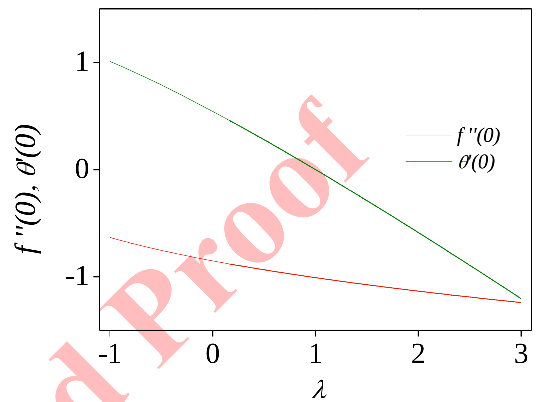

Figure 8. Variation of wall shear stress ($f''(0)$) and Nusselt number ($\theta'(0)$) values as a function of velocity ratio parameter λ for $Pr = 1,\ \beta = 0.5, K = 0.25,\ N = 1$.

5. Conclusions

We have presented the forced convective heat transfer and boundary layer flow of a Newtonian fluid over a wedge in which the velocity-slip is also accounted in the study. We have transformed the governing equations to a system of first order nonlinear ordinary differential equations and have solved numerically using Keller-box method. The various results on velocity, temperature profiles and wall-shear stress and temperature gradients are presented. Our numerical results show that the thicknesses of momentum (thermal) boundary layer are found to be thinner (thicker) for increasing unsteady, pressure gradient and velocity ratio parameters. While the thickness for both boundary layers is thinner for increasing velocity-slip parameter. Further, the velocity and temperature gradients on the wall are found to increase for unsteadiness of the flow and the opposite trend is noticed for velocity-slip parameter. The effect of velocity-slip is to enhance the heat transport in the boundary layer by transferring some of wedge heat to the fluid.

Acknowledgments

Authors would like to thank the Editor and an anonymous reviewer for the useful comments which improved the quality of the article.

References

[1] T. A. Abdelhafez, *Skin friction and heat transfer on a continuous flat surface moving in a parallel free stream*, International Journal of Heat and Mass Transfer, *28* (1985), 1234-1237.

[2] N. Afzal, A. Badaruddin, and A. A. Elgarvi, *Momentum and heat transport on a continuous flat surface moving in a parallel stream*, International Journal of Heat and Mass Transfer, *36* (1993), 3399-3403.

[3] M. T. Akolade, *Thermo-physical impact on the squeezing motion of non-Newtonian fluid with quadratic convection, velocity slip, and convective surface conditions between parallel disks*, Partial Differential Equations in Applied Mathematics, *4* (2021), 100056.

[4] P. D. Ariel, T. Hayat, and S. Asghar, *The flow of an elastico-viscous fluid past a stretching sheet with partial slips*, Acta Mechanics, *187* (2006), 29-35.

[5] N. Bachok, A. Ishak, and I. Pop, *Melting heat transfer in boundary layer stagnation-point flow towards a stretching/shrinking sheet*, Physics Letters A, *374* (2010), 4075-4079.

[6] G. K. Batchelor, *An introduction to fluid dynamics*, first ed., Cambridge University Press, (1967).

[7] K. Bhattacharyya, S. Mukhopadhyay, and G. C. Layek, *MHD boundary layer slip flow and heat transfer over a flat plate*, Chinese Physics Letters, *28* (2011), 024701-024704.

[8] K. Cebeci and P. Bradshaw, *Momentum transfer in boundary layers*, Mc-Graw Hill, New York, (1977).

[9] N. V. Churaev, V. D. Sobolev, and N. Somov, *Slippage of liquids over lyophobic solid surfaces*, Journal of Colloidal and Interface Science, *97* (1984), 574-581.

[10] V. S. J. Craig, C. Neto, and D. R. M. Williams, *Shear-dependent boundary slip in an aqueous Newtonian liquid*, Physical Review Letters, *87* (2001), 054504/1-4.

[11] L. J. Crane, *Flow past a stretching plate*, Journal of Applied Mathematics and Physics, *21* (1970), 645-647.

[12] P. W. Duck and S. L. Dry, *On a class of unsteady, nonparallel, three-dimensional disturbances to boundary-layer flows*, Journal of Fluid Mechanics, *441* (2001), 31-65.

[13] P. W. Duck, S. R. Stow, and M. R. Dhanak, *Boundary-layer flow along a ridge: alternatives to the Falkner-Skan solutions*, Philosophical Transactions of the Royal Society A, *358* (2000), 3075-3090.

[14] R. Ellahi, S. Z. Alamri, A. Basit, and A. Majeed, *Effects of MHD and slip on heat transfer boundary layer flow over a moving plate based on specific entropy generation*, Journal of Taibah University for Science, *12* (2016), 476-482.

[15] T. Grosan and I. Pop, *Forced convection boundary layer flow past non-isothermal thin needles in nanofluids*, ASME-Journal of Heat Transfer, *133* (2011), 054503.

[16] S. P. Hastings and W. C. Troy, *Oscillating solutions of the Falkner-Skan equation for negative β*, SIAM Journal on Mathematical Analysis, *18* (1987), 422-429.

[17] W. Ibrahim and B. Shanker, *Magnetohydrodynamic boundary layer flow and heat transfer of a nanofluid over non-isothermal stretching sheet*, ASME-Journal of Heat Transfer, *136* (2014), 051701.

[18] K. Kaladhar, K. Madhusudhan Reddy, and D. Srinivasacharya, *Inclined magnetic field and Soret effects on mixed convection flow between vertical parallel plates*, Journal of Applied Analysis and Computation, *9*(6) (2019), 2111-2123.

[19] H. B. Keller, *Numerical methods in boundary layer theory*, Annual Review of Fluid Mechanics, *10* (1978), 417-428.

[20] W. A. Khan and I. Pop, *Free convection boundary layer flow past a horizontal flat plate embedded in a porous medium filled with a nanofluid*, ASME-Journal of Heat Transfer, *133* (2011), 094501.

[21] R. B. Kudenatti, N. E. Misbah, and M. C. Bharathi, *Linear Stability of Momentum Boundary Layer Flow and Heat Transfer Over a Moving Wedge*, Journal of Heat Transfer-Transactions of the ASME, *142*(6) (2020), 061804.

[22] M. K. Mishra, G. S. Seth, and R. Sharma, *Navier's slip effect on mixed convection flow of non-Newtonian nanofluid: Buongiorno's model with passive control approach*, International Journal of Applied and Computational Mathematics, *5* (2019), 107.

[23] S. Mukhopadhyay and R. S. R. Gorla, *Effects of partial slip on boundary layer flow past a permeable exponential stretching sheet in presence of thermal radiation*, Heat and Mass Transfer, *48* (2012), 1773-1781.

[24] S. Mukhopadhyay, *Slip effects on MHD boundary layer flow over an exponentially stretching sheet with suction/blowing and thermal radiation*, Ain Shams Engineering Journal, *4* (2013), 485-491.

[25] A. Nakayama, Kokudai, and H. Koyama, *Non-Darcian boundary layer flow and forced convective heat transfer over a flat plate in a fluid-saturated porous medium*, ASME-Journal of Heat Transfer, *112* (1990), 157-162.

[26] C. L. Navier and M. H. Memoire, *Sur les lois du mouvement des fluids*, Mem. Academic Science Institute of France, *6* (1823), 389–440.

[27] B. Oskam and A. E. P. Veldman, *Branching of the Falkner-Skan solutions for $\lambda < 0$*, Journal of Engineering Mathematics, *16* (1982), 295-308.

[28] A. Parmar and S. Jain, *Exploration of heat and mass transfer in the convective slip flow of non-Newtonian Casson fluid*, International Journal of Applied and Computational Mathematics, *4* (2018), 67.

[29] J. Rao and K. R. Rajagopal, *The effect of the slip boundary condition on the flow of fluids in a channel*, Acta Mechanica, *135* (1999), 113–126.

[30] P. L. Sachdev, R. B. Kudenatti, and N. M. Bujurke, *Exact analytic solution of boundary value problem for the Falkner-Skan equation*, Studies in Applied Mathematics, *120* (2008), 1-16.

[31] B. C. Sakiadis, *Boundary-layer behavior on continuous solid surfaces*, Journal of AICHE, *7* (1961), 26-28.

[32] M. Z. Salleh, R. Nazar, and I. Pop, *Forced convection boundary layer flow at a forward stagnation point with Newtonian heating*, Chemical Engineering Communications, *196* (2009), 987-996.

[33] S. R. Sayyed, B. B. Singh, and B. Nasreen, *Analytical solution of MHD slip flow past a constant wedge within a porous medium using DTM-Pade*, Applied Mathematics and Computation, *321* (2018), 472-482.

[34] H. Schlichting and K. Gersten, *Boundary Layer Theory*, 8th ed., Springer, New York, 2004.

[35] M. Sheikholeslami and A. J. Chamkha, *Influence of Lorentz forces on nanofluid forced convection considering Marangoni convection*, Journal of Molecular Liquids, *225* (2017), 750-757.

[36] M. Sheikholeslami, H. R. Kataria, and A. S. Mittal, *Effect of thermal diffusion and heat-generation on MHD nanofluid flow past an oscillating vertical plate through porous medium*, Journal of Molecular Liquids, *257* (2018), 12-25.

[37] C. Y. Wang, *Analysis of viscous flow due to a stretching sheet with surface slip and suction, Nonlinear Analysis: Real World Applications*, *10* (2009), 375-380.

[38] H. T. Yang and L. C. Chien, *Analytic solutions of the Falkner-Skan equation when β = -1 and γ = 0*, SIAM Journal on Applied Mathematics, *29* (1975), 558-569.